Cell Respiration Under Hypoxia: Facts and Artefacts in Mitochondrial Oxygen Kinetics

Francesca M. Scandurra and Erich Gnaiger

Abstract When oxygen supply to tissues is limiting, mitochondrial respiration and ATP production are compromised. To assess the bioenergetic consequences under normoxia and hypoxia, quantitative evaluation of mitochondrial oxygen kinetics is required. Using high-resolution respirometry, the "apparent K_m" for oxygen or p_{50} of respiration in 32D cells was determined at 0.05 ± 0.01 kPa (0.4 mmHg, 0.5 μM, 0.25% air saturation). Close agreement with p_{50} of isolated mitochondria indicates that intracellular gradients are small in small cells at routine activity. At intracellular $p_{O_2} < 2$ kPa (15 mmHg, 10% air saturation) in various tissues under normoxia, respiration is limited by >2% with a p_{50} of 0.05 kPa. Over-estimation of p_{50} at 0.4 kPa (3 mmHg) would imply significant (>17%) oxygen limitation of respiration under intracellular normoxia. Based on a critical review, we conclude that p_{50} ranges from 0.01 to 0.10 kPa in mitochondria and small cells in the absence of inhibitors of cytochrome *c* oxidase, whereas experimental artefacts explain the controversial >200-fold range of p_{50} in the literature on mitochondrial oxygen kinetics.

1 Introduction

Intracellular oxygen levels in the microenvironment of mitochondria are the result of a dynamic balance between oxygen transport to tissues through the respiratory cascade [1] and oxygen utilization by the mitochondrial respiratory electron transport system [2]. At any physiological steady state, a metabolic perturbation of oxygen demand leads to a shift of intracellular oxygen concentration (decrease after stimulation or increase after arrest), unless effective control of oxygen supply exerts a compensatory effect to maintain intracellular oxygen levels within a regulated range. Conversely, an environmental

E. Gnaiger (✉)
D. Swarovski Research Laboratory, Department of General and Transplant Surgery, Medical University of Innsbruck, Innsbruck, Austria; OROBOROS INSTRUMENTS, Innsbruck, Austria
e-mail: erich.gnaiger@i-med.ac.at

E. Takahashi, D.F. Bruley (eds.), *Oxygen Transport to Tissue XXXI*, Advances in Experimental Medicine and Biology 662,
DOI 10.1007/978-1-4419-1241-1_2,

perturbation from normoxic to hypoxic or hyperoxic levels modifies the variables of oxygen transport and the metabolic capacity for oxygen consumption is compromised if mitochondrial oxygen pressures are changed below the level of kinetic saturation. Three elements, therefore, are responsible for controlling cellular oxygenation: the environmental oxygen level, oxygen transport and respiratory metabolism.

This review is focused on cellular and mitochondrial respiration, under the control of extracellular or mitochondrial oxygen pressure (Section 2). In Section 3, we summarize our experience gained by application of high-resolution respirometry to the study of isolated mitochondria and intact cells under conditions of varying oxygen concentrations. Extending the comprehensive review on mitochondrial oxygen kinetics published in 1995 [3], we discuss in Section 4 possible explanations for discrepancies on the p_{50} of mitochondrial respiration, i.e. the partial pressure at which respiration rate is 50% of flux at kinetic oxygen saturation. There is a >200-fold range of mitochondrial p_{50} reported in the literature. Whereas instrumental and methodological artefacts are responsible for the major part of this large range, a 10-fold variation of p_{50} is due to turnover of cytochrome *c* oxidase (between the minimum of respiration compensating for leak and fully ADP-stimulated respiration) and variation between different mitochondrial sources and various small cells. In Section 5, we relate the p_{50} of mitochondrial respiration to intracellular oxygen regimes under normoxia and hypoxia, discussing the theoretical consequences of the actual p_{50} of mitochondrial respiration under physiological conditions, for energy homeostasis and mitochondrial excess capacities, oxygen sensing and signalling responses to hypoxia. In particular, comparison of the p_{50} in isolated mitochondria and intact cells supports the direct measurement of high intracellular oxygen gradients in cardiomyocytes [4, 5], in contrast to the comparatively negligible intracellular oxygen gradients in small cells [6].

2 Mitochondrial and Cellular Oxygen Kinetics

2.1 Isolated Mitochondria

Mitochondrial respiration is a hyperbolic function of oxygen partial pressure, p_{O_2},

$$j_{O_2} = \frac{p_{O_2}}{p_{50} + p_{O_2}} \tag{1}$$

where j_{O_2} is the rate expressed relative to the maximum pathway flux, J_{max}, observed at kinetic oxygen saturation in a defined metabolic state. Characteristic metabolic states of isolated mitochondria, incubated with selected substrate combinations (e.g. pyruvate, malate, glutamate, succinate), are (i) *OXPHOS* (State 3 [7]; maximally ADP-stimulated oxidative phosphorylation; but see [8]), and (ii) *LEAK* (State 4 [7]; minimum oxygen flux required to compensate for proton leak,

slip and cation cycling, without providing ADP or by inhibiting phosphorylation; for discussion see [9]). J_{max}, therefore, is a complex function of coupling and electron supply through the mitochondrial electron transport system to cytochrome *c* oxidase. Similarly, the maximum reaction velocity of an enzyme, V_{max}, varies as a function of the concentrations of other substrates and enzyme concentration, [E]. The enzyme turnover, $V_{max}/[E]$, or pathway flux, J_{max}, exert an influence on the apparent Michaelis-Menten constant, K_m', or p_{50}. The p_{50} of mitochondrial respiration, therefore, depends on the metabolic state. If catalytic efficiency, V_{max}/K_m', is constant, then K_m' and p_{50} increase in direct proportion to enzyme turnover [10]. In addition to substrate and ADP supply [11], coupling of electron transport to phosphorylation modifies the p_{50} of cellular and mitochondrial respiration [2, 12, 13]. Since the present review is focussed on mitochondrial physiology, we will not consider uncoupled states which provide a measure of the capacity of the electron transport system, *ETS*.

2.2 Intact Cells

In the *ROUTINE* state, cell respiration is controlled by physiological aerobic ATP demand at routine steady-state ADP levels, which result from the dynamic balance of ATP production (aerobic and glycolytic) and cellular ATP utilization. After inhibition of electron transport, e.g. by 0.5 μM myxothiazol, residual oxygen consumption (*ROX*) is observed which is subtracted from total oxygen consumption to obtain mitochondrial *ROUTINE* respiration. As shown by the inhibitory effect of oligomycin, which inhibits ATP synthase and induces a *LEAK* respiratory state, *ROUTINE* respiration is about two to four times higher than *LEAK* respiration, and is thus significantly less than *OXPHOS* capacity, which may be six to ten times the *LEAK* respiration, as expressed by the respiratory control ratio [14, 15].

In addition to the enzymatically catalyzed oxygen consumption, the oxygen dependence of cell respiration is controlled by oxygen gradients related to oxygen transport from the extracellular medium to the mitochondria. The oxygen pressure difference, Δp_{cell}, between the extracellular medium and the average mitochondrion is a function of cell size, cell shape, mitochondrial distribution and oxygen flux. At half-maximum oxygen flux, oxygen gradients are 50% of their maximum at unlimited flux, and maximum $\Delta p_{cell} = 2 \cdot \Delta p_{50}$ can be calculated as the p_{50} difference of respiration in intact cells and isolated mitochondria, at comparable metabolic states [6],

$$\Delta p_{50} = p_{50,cell} - p_{50,mito} \tag{2}$$

For comparison of mitochondria and cells, respiration is expressed as oxygen flux per mitochondrial protein, J_{O_2} [pmol·s^{-1}·mg^{-1}], or relative to a mitochondrial marker such as aa_3 content or citrate synthase activity. Cell respiration is frequently expressed as oxygen flow per number of cells, I_{O_2} [pmol·s^{-1}·10^{-6}], which is an extensive quantity and varies with cell size and

mitochondrial content [16]. High oxygen flow in large and active cells, such as cardiomyocytes, results in proportionally high Δp_{50} [6].

3 Oxygen Kinetics and High-Resolution Respirometry

3.1 Nanomolar Resolution of Oxygen Concentration

Measurement of mitochondrial oxygen kinetics presents an experimental challenge [3, 17, 18], considering the demands set on oxygen monitoring with high sensitivity and high time resolution. High-resolution respirometry (HRR) was developed for routine measurement of low volume-specific oxygen flux and low, sub-micro molar oxygen concentration [3]. The instrumental and methodological basis of HRR (Oxygraph-2 k; OROBOROS INSTRUMENTS, Austria; www.oroboros.at) has been discussed in detail [11]. Since 2001, HRR was improved further in a second generation of instruments (Oxygraph-2 k) with reduced signal noise (Fig. 1; compare Fig. 3) as achieved by higher temperature stability, improved stirring and advanced electronics and mechanical design. The HRR features most important for oxygen kinetics are summarized briefly: (1) The experimental chamber and sealings are made of inert materials which do not store and release dissolved oxygen (no Perspex, no Teflon coated stirrers). (2) Unstirred layers are minimized by effective stirring, and gas-aqueous phase

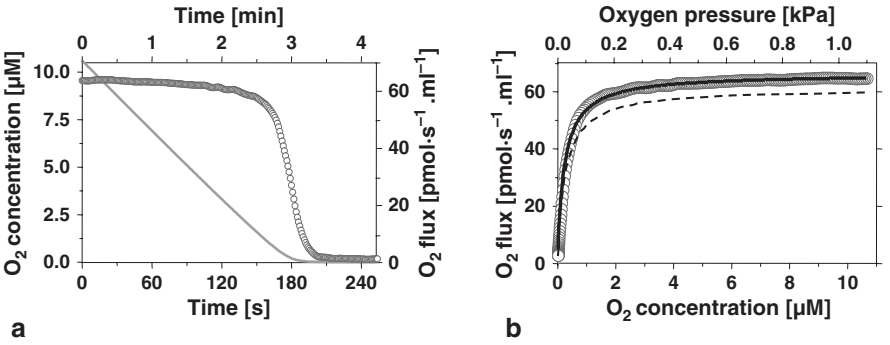

Fig. 1 Oxygen kinetics of respiration of 32D cells in a closed chamber (2 ml mitochondrial respiration medium MiR05; OROBOROS Oxygraph-2 k; $5{\cdot}10^6$ cells·ml^{-1}, 37°C). **a**. Oxygen concentration (*continuous line*) and volume-specific oxygen flux (*circles*) as a function of time during the aerobic-anoxic transition. The oxygen signal was corrected for the time constant ($\tau = 2.8$ s) of the O_2 sensor. Oxygen flux was corrected for instrumental background. **b**. Hyperbolic fit (*continuous line*) in the low-oxygen range of oxygen flux (*circles*) as a function of oxygen concentration or oxygen pressure (oxygen solubility 9.71 µM/kPa). Maximum flux, $J_{V,\max}$, was 66 pmol·s^{-1}·ml^{-1}. Corresponding to the low maximum flow, $I_{\max}$, of 13 pmol·s^{-1}·ml^{-1} in the endogenous *ROUTINE* state, the p_{50} was 0.028 kPa (0.21 mmHg; 0.27 µM). After re-oxygenation and dilution of the cells by a factor of 0.94–$4.7{\cdot}10^6$ cells·ml^{-1} (due to injections of aerobic respiration medium; not shown), respiratory flow (per cell) returned to the initial value, and the p_{50} was 0.022 kPa in a second aerobic-anoxic transition (dashed line, showing the lower volume-specific flux at the lower cell density)

boundaries are avoided to exclude uncontrolled oxygen gradients. (3) Polarographic oxygen sensors (POS) with a large cathode, inserted into the precisely thermostated O2k-chamber (±0.001°C) yield a linear signal with low noise over a 500,000-fold dynamic range. Noise decreases with declining oxygen pressure, which eliminates the requirement for smoothing in the low-oxygen range and ensures high time resolution. (4) Accurate oxygen calibrations are obtained at air saturation and zero oxygen concentration, with correction for signal drift in the nanomolar concentration range. (5) High digital resolution (2 nM) and data recording at intervals of one second are a basis for deconvolution of the oxygen signal with the calibrated first-order exponential time constant of the POS, and for calculating oxygen flux, J_{V,O_2} [pmol·s^{-1}·ml^{-1}], as the time derivative of oxygen concentration. (6) Errors of oxygen flux are minimized by on-line correction for instrumental background, calibrated by measurement of residual oxygen back-diffusion into the system and oxygen consumption by the POS over the entire experimental oxygen range. (7) Concentrations of mitochondria or cells are varied in a range compatible with instrumental sensitivity, time resolution and steady-state enzyme kinetics. In this range, measurement of p_{50} must be independent of sample concentration or transition time. (8) Before aerobic-anoxic transitions, oxygen flux must be sufficiently stable to exclude time effects superimposed over oxygen dependence of respiration. In addition, reversibility and stability of respiration are evaluated after re-oxygenation, which is particularly important in prolonged experiments with steady-state oxygen levels. (9) By selecting oxygen pressures <1.1 kPa for hyperbolic analysis [3], oxygen levels >10 times the p_{50} are covered, without extending to non-physiological high oxygen pressures. (10) Non-linear hyperbolic fits of the flux/oxygen pressure relation are tested by evaluation of residuals rather than linearity of double-reciprocal plots [19].

3.2 High-Resolution Oxygen Kinetics: Effects of Cell Density and Cell Activity

Mouse parental promyeloid 32D cells [20] are small cells grown in suspension in RPMI 1640 (PAA Laboratories Pasching, Austria). Figure 1a shows typical traces of oxygen concentration and oxygen flux during an aerobic-anoxic transition. Flux was a hyperbolic function of oxygen concentration with a p_{50} of 0.028 and 0.022 kPa in the first and second transition, at I_{max} of 13 pmol·s^{-1}·10^{-6} (Fig. 1b). Oxygen flow of intact 32D cells varied between cultures, with identical or occasionally very low activities of cells incubated in mitochondrial respiration medium MiR05 (compared to cell culture medium RPMI; Fig. 2a). The "intracellular" mitochondrial respiration medium is not physiological, but is frequently used in respiratory studies with cells, when plasma membrane permeabilization is effected as part of the titration protocol in the Oxygraph-2 k chamber [16]. The lowest values of oxygen flow in MiR05 are representative of an inactive respiratory state, as shown by comparison with oligomycin-inhibited respiration of cells measured in RPMI (Fig. 2a). In Fig. 2b, p_{50} values from the same experiments are plotted against volume-

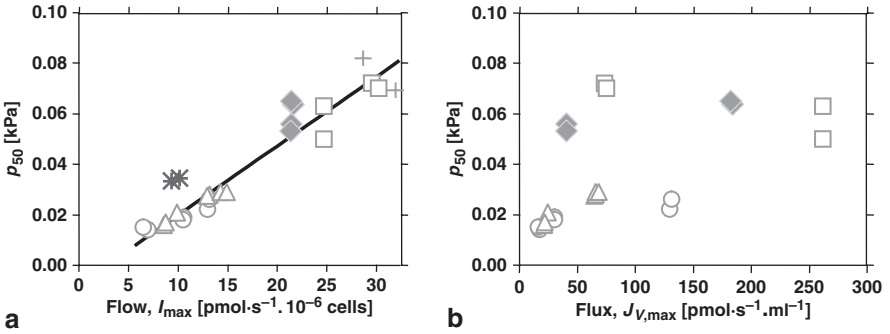

Fig. 2 Oxygen kinetics of respiration of 32D cells incubated in cell culture medium RPMI (*full symbols*) or mitochondrial respiration medium MiR05 (*open symbols*). **a**. Dependence of p_{50} on oxygen flow (per 10^6 cells). * and + indicate averages from two parallel determinations of *ROUTINE* and *LEAK* respiration, respectively, with 32D-vRAF cells. **b**. Independence of p_{50} on oxygen flux (per ml of cell suspension), in paired experiments at two dilutions of cell concentration [x10^6 cells/ml]: 2.5 and 5.0 (*triangles*); 2.9 and 10.0 (*circles*); 2.5 and 10.6 (*squares*); 1.9 and 8.5 (*diamonds*). Each symbol indicates a single aerobic-anoxic transition

specific *ROUTINE* oxygen flux, which was varied from 16 to 260 pmol·s^{-1}·ml^{-1} by incubation of each cell culture at two different cell concentrations in the range of $2 \cdot 10^6$–$11 \cdot 10^6$ cells/ml. Cell density exerts its effect not only on volume-specific flux, $J_{V,max}$, but may also modulate cell-specific oxygen flow, I_{max} (for HUVEC, see [12]). As reported previously [12, 13, 18], variation of mitochondrial or cell density provides an essential test for instrumental time resolution and kinetic consistency of p_{50} values.

Variation of oxygen flow (per cell; Fig. 2a) in paired experiments with the same cell culture (Fig. 2b) was due to different levels of activity in the *ROUTINE* state. The corresponding range in turnover of cytochrome *c* oxidase explains the linear dependence of p_{50} on cell respiration (Fig. 2a). Variation of cell size and mitochondrial content provides an alternative mechanism for variation of respiratory activity per cell [16]. At constant mitochondrial p_{50} (constant turnover of cytochrome *c* oxidase), however, cellular p_{50} would not vary with oxygen flow per cell, except if intracellular gradients and Δp_{50} (Eq. 2) increase with cell size in different cultures.

The linear increase of p_{50} as a function of oxygen flow (per cell; Fig. 2a) indicates varying enzyme turnover at constant mitochondrial content per cell, which was further supported by the constant citrate synthase activity per cell (data not shown). Additional support for our interpretation in terms of variation of mitochondrial activity stems from independent control experiments with 32D-vRAF cells suspended in RPMI and pharmacological intervention with respiratory activity. When *ROUTINE* respiration was inhibited by oligomycin (2 μg/ml), the p_{50} declined proportional to the reduced *LEAK* respiratory flow. These results are comparable to the decrease of p_{50} in isolated mitochondria from the active *OXPHOS* state to the passive *LEAK* state ([2, 13, 21]; Table 1).

Table 1 p_{50} of mitochondrial respiration in different metabolic states of coupled respiration (*LEAK*: resting, not ADP-activated; *OXPHOS*: active, ADP-activated; *ROUTINE*: under physiological control of activation in intact cells). Respiratory flux at kinetic oxygen saturation, J_{max}, is expressed in pmol/(s·unit x); if unit x is cell number, then J_{max} becomes I_{max}. J_{Vmax} is flux per volume of incubation medium. **A**: p_{50} in isolated mitochondria (mt) and small cells. **B**: Results in closed systems with J_{Vmax} above 500 pmol·s^{-1}·ml^{-1} [13], and in closed and open systems with apparent problems of oxygen heterogeneity. **C**: p_{50} based on intracellular p_{O_2} reported by myoglobin in large muscle cells and tissues

Model [1,2]	T (°C)	J_{max} (pmol/(s·x))	Unit [3]X	Density (x/ml)	J_{Vmax} (pmol/(s·ml))	p_{50} (kPa)	Exp.[4]	Ref.
A.								
LEAK								
Beef HMmt	25	–	–	–	52	0.005	C	1965 [10]
RLmt, GS	25	–	–	–	42	0.004	C	1965 [10]
Pigeon HMmt, GS	25	–	–	–	19	0.002	C	1965 [10]
RHMmt, GM	25	465	Nmol *c*	0.2	93	0.032	C	1990 [18]
RHMmt, GMS	25	1170	Nmol *c*	0.2	234	0.048	C	1990 [18]
RLmt, S(Rot)	25	210	mg P_{mt}	0.6	126	0.025	C_{HRR}	1994 [31]
RSMmt, GM	37	–	–	–	170	0.025	C_{HRR}	1995 [3]
RLmt, S(Rot)	37	210	mg P_{mt}	0.6	126	0.025	C_{HRR}	1995 [3]
RLmt, S(Rot)	25	170	mg P_{mt}	0.5	85	0.028	C_{HRR}	1997 [32]
RHMmt, PM	25	190	mg P_{mt}	0.5	95	0.023	C_{HRR}	1997 [32]
RHMmt, PM	30	590	mg P_{mt}	0.12	71	0.016	C_{HRR}	1998 [2]
RLmt, S(Rot)	30	280	mg P_{mt}	0.5	140	0.02	C_{HRR}	1998 [2]
RLmt, S(Rot)	25	210	mg P_{mt}	0.58	122	0.024	C_{HRR}	2000 [27]
Artemia Emt, S(Rot)	25	223	mg P_{mt}	0.26	58	0.057	C_{HRR}	2000 [27]
Frog SMmt, PM	20	82.6	mg P_{mt}	1	83	0.024	C_{HRR}	2000 [28]
Frog SMmt, PM	3	20	mg P_{mt}	1	20	0.005	C_{HRR}	2000 [28]
32D-vRaf, RPMI, Omy	37	10	10^6 cells	$6 \cdot 10^6$	60	0.034	C_{HRR}	Fig. 2
Pigeon HMmt, GS	25	530	mg P_{mt}	0.2	106	0.008	O	1974 [21]
RLmt, S(Rot)	25	210	mg P_{mt}	0.21	42	0.02	O_{HRR}	2000 [11]
OXPHOS								
RLmt, S	26	–	mg P_{mt}	0.2	–	0.015	C	1970 [51]
Beef Amt, S	26	–	mg P_{mt}	0.2	–	0.024	C	1970 [51]

Table 1 (continued)

Model [1,2]	T (°C)	J_{max} (pmol/(s·x))	Unit [3]X	Density (x/ml)	J_{Vmax} (pmol/(s·ml))	p_{50} (kPa)	Exp.[4]	Ref.
Yeast mt, PM	25	–	mg P_{mt}	0.2	–	0.04	C	1970 [51]
RHMmt	30	4500	mg P_{mt}	0.1	450	0.035	C_{HRR}	1998 [2]
RLmt, S(Rot)	30	1240	mg P_{mt}	0.3	372	0.057	C_{HRR}	1998 [2]
Frog SMmt, PM	20	420	mg P_{mt}	1	420	0.052	C_{HRR}	2000 [28]
Frog SMmt, PM	3	89	mg P_{mt}	1	89	0.015	C_{HRR}	2000 [28]
RLmt, PM	–	110	mg P_{mt}	6	660	0.05	O	1971 [52]
Pigeon HMmt, GS	25	2900	mg P_{mt}	0.2	580	0.08	O	1974 [21]
ROUTINE								
Yeast, ethanol	25	–	–	–	–	0.035	C	1965 [10]
CHP-404	–	79	mg W_d	5	395	0.110	C	1989 [53]
IMR-5	–	68	mg W_d	5	340	0.103	C	1989 [53]
HUVEC, EGM	37	45	10^6 cells	2	90	0.063	C_{HRR}	1994 [54]
HUVEC, M199	37	20	10^6 cells	2	40	0.094	C_{HRR}	1994 [54]
HUVEC, EGM	37	40	10^6 cells	2	125	0.075	C_{HRR}	1996 [12]
Platelets	37	0.1	10^6 cells	1500	149	0.082	C	1999 [48]
Fibroblast	37	49.6	10^6 cells	1.5	74	0.082	C_{HRR}	2002 [24]
Fibroblast	37	60.5	mg P_c	0.7	42	0.039	C_{HRR}	2004 [25]
32D-vRAF, RPMI	37	30	10^6 cells	6	180	0.076	C_{HRR}	Fig. 2
32D cells; RPMI	37	18	10^6 cells	10	180	0.051	C_{HRR}	Fig. 2
Rat coronary EC	37	65	mg P_c	–	–	0.110	O	1990 [55]
Sunflower leaves	22	60	cm^2	–	–	0.041	O	2007 [26]
Aspen leaves	22	100	cm^2	–	–	0.059	O	2007 [26]
B.								
LEAK								
RLmt, GS	25	670	mg P_{mt}	1.0	670	0.060	C	1988 [56]
RHMmt, GMS	25	1158	nmol *c*	0.8	926	0.051	C	1990 [18]
RLmt, S(Rot)	37	333	mg P_{mt}	1.0	–	0.333	O_{GAP}	2007 [38]

Table 1 (continued)

Model [1,2]	T (°C)	J_{max} (pmol/(s·x))	Unit [3]X	Density (x/ml)	J_{Vmax} (pmol/(s·ml))	p_{50} (kPa)	Exp.[4]	Ref.
OXPHOS								
RLmt, S(Rot)	25	1780	mg P_{mt}	0.5	890	0.157	C_{HRR}	1997 [32]
RHMmt, PM	25	1550	mg P_{mt}	0.5	775	0.135	C_{HRR}	1997 [32]
RSMmt, GM	25	1500	mg P_{mt}	10	15000	0.005	O_{GAP}	1982 [37]
RLmt, S(Rot)	37	–	mg P_{mt}	1	–	0.258	O_{GAP}	2003 [39]
RLmt, S(Rot)	37	1833	mg P_{mt}	1	1833	0.278	O_{GAP}	2007 [38]
ROUTINE								
Jurkat cells	37	19.2	10^6 cells	26	500	0.245	C	2003 [34]
HUVEC, L-NMMA	37	–	10^6 cells	31	~1000	0.436	C	2004 [33]
RAW 246.7, L-NMMA	37	18	10^6 cells	52	937	0.309	C	2004 [33]
BAEC	37	10	10^6 cells	2	20	0.153	C_u	2006 [35]
BAEC	37	10	10^6 cells	3	31	0.247	C_u	2006 [35]
BAEC	37	16	10^6 cells	5	78	0.340	C_u	2006 [35]
BAEC	37	159	10^6 cells	8	1276	0.631	C_u	2008 [57]
BAEC, stress	37	73	10^6 cells	8	580	0.340	C_u	2008 [57]
C.								
RH myocytes	30	91	mg P_c	0.3	27	0.015	O_{GAP}	1985 [43]
Perfused RH	25	160	mg W_d	–	–	0.070	P	1995 [40]
Human SM	37	–	–	–	–	0.2	P	1999 [41]
Mouse SM	37	6.86	mg W_w	–	–	0.16	P	2003 [42]

(1) Mitochondria (mt): 32D (32D-vRaf), murine promyeloid cells (over-expressing the *v*-Raf gene); *Artemia* E, *Artemia franciscana* embryo; Amt, adrenocortical mt; BAEC, bovine aortic endothelial cells; BAEC stress, after shear stress; CHP-404, neuroblastoma cell line; EC, endothelial cells; HM, heart muscle; HUVEC, human umbilical vein endothelial cells; IMR-5, neuroblastoma cell line; Jurkat cells, human leukocytes; RAW 246.7, murine monocytic cell line; RH, rat heart; RHM, rat heart muscle; RL, rat liver; RSM, rat skeletal muscle; SM, skeletal muscle.
(2) Substrates, inhibitors and media: *c*, cytochrome *c*; EGM, endothelial growth medium; G, glutamate; L-NMMA, N^G-monomethyl-L-arginine monoacetate; M, malate; M199, growth medium; Omy, oligomycin; P, pyruvate; Rot, rotenone; RPMI, growth medium; S, succinate.
(3) Unit [mg]: P_c, cell protein; P_{mt}; mitochondrial protein; W_d, dry weight; W_w, wet weight.
(4) Experimental system: C, closed; C_{HRR}, closed high-resolution respirometry; C_u, closed unstirred; O, open; O_{GAP}, open with the gas-aqueous phase system of [37]; O_{HRR}, open high-resolution respirometry; P, perfused organ including measurement in vivo.

A linear dependence of the K_m' of cytochrome *c* oxidase on enzyme turnover [10] was shown conclusively in the bacterial enzyme [22, 23].

Respiratory flow in the *ROUTINE* state of 32D cells in RPMI averaged 18.4 ± 3.7 pmol·s^{-1}·10^{-6} ($N = 39$; compare [15]), and the corresponding p_{50} was 0.051 ± 0.012 kPa (= 0.38 mmHg; $c_{50} = 0.48$ μM; Table 1). The 32D cell volume is 0.0009 ± 0.0001 mm^3 (0.9 pL), determined in a CASY1 TT system (Schärfe System, Reutlingen, Germany). These cells are comparable to human umbilical vein endothelial cells (HUVEC) in terms of cell volume, *ROUTINE* respiration, electron transport capacity after uncoupling and p_{50} [12, 15].

We have not determined the oxygen kinetics of mitochondria isolated from 32D cells, but may compare the cellular p_{50} with results on mitochondria isolated from rat liver and rat heart, which is 0.016 and 0.020 kPa in the passive *LEAK* state and 0.035 and 0.057 kPa in the active *OXPHOS* state with substrates for Complex I or succinate + rotenone for Complex II ([2, 13]; Fig. 3a, b). Since the substrate combination for Complex I + II exerts an additive effect and stimulates *OXPHOS* capacity to a higher level of cytochrome *c* oxidase turnover [9], the p_{50} in the active *OXPHOS* state of Complex I- or Complex

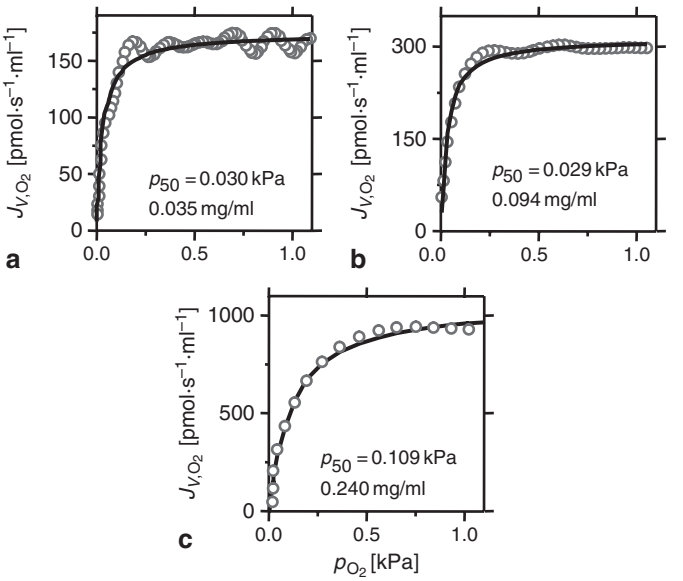

Fig. 3 Oxygen flux per volume of incubation medium, J_{V,O_2} [pmol·s^{-1}·ml^{-1}], as a function of oxygen pressure, p_{O_2}, in the low-oxygen range <1.1 kPa, in active heart mitochondria (*OXPHOS*, 1 mM ADP, 1 mM ATP, 2 mM pyruvate, 5 mM malate; 30°C), at different mitochondrial protein concentrations [mg/ml]. Protein-specific flux at kinetic oxygen saturation, J_{max}, is 4.5 nmol·s^{-1}·mg^{-1} independent of protein concentration. Similarly, the p_{50} is independent of protein concentration (**a** and **b**), whereas the increase of p_{50} (**c**) is an experimental artefact at protein concentrations >0.15 mg/ml, corresponding to volume-specific J_{max} >500 pmol·s^{-1}·ml^{-1}. From [13]

II-respiration is quite comparable to turnover conditions in the *ROUTINE* state. Taken together, these data indicate that the small intracellular oxygen gradients (Eq. 2) in 32D cells are close to the limit of detection. Similar conclusions are drawn [6] from the oxygen kinetics of HUVEC (*ROUTINE* $I_{O_2} = 30–50$ pmol·s^{-1}·10^{-6} and $p_{50} = 0.05–0.08$ kPa [12]) and human fibroblasts (*ROUTINE* $I_{O_2} = 50$ pmol·s^{-1}·10^{-6} and $p_{50} = 0.04–0.08$ kPa [24, 25], where oxygen flow, I_{O_2}, is given per number of cells).

4 Discussion

4.1 Comparative Mitochondrial Physiology and p_{50} of Mitochondrial Respiration

Extending previous reviews on oxygen kinetics of mitochondrial respiration [3, 6], Table 1A and Fig. 4 summarize p_{50} and respiration in isolated, coupled mitochondria incubated with physiological substrates and in intact small cells. With a focus on mitochondrial physiology, no data are included on (i) uncoupled respiration [3, 12, 13, 18]; (ii) the isolated step of cytochrome *c* oxidase with artificial substrates, and (iii) large cells (hepatocytes, cardiomyocytes) where oxygen gradients are significant [4, 6]. In addition to rat liver, rat heart and various mammalian cell types, a large variety of mitochondrial sources has been tested, including plants [26], brine shrimp embryos (*Artemia* [27]), and frog skeletal muscle [28]. Considering this broad spectrum of comparative mitochondrial physiology and respiratory states from *LEAK* to *ROUTINE* and *OXPHOS*, the range of p_{50} from 0.01 to 0.11 kPa (0.08–0.75 mmHg) is remarkably consistent, and independent of measurement in closed or open chambers if methodological criteria are met as summarized above (Section 3.1; [3]).

Close agreement of p_{50} for small cells and isolated mitochondria suggests that Δp_{50} (Eq. 2) is in the order of 0.01–0.03 kPa (Table 1A). A 10- to 20-fold higher Δp_{cell} has been reported by delayed fluorescence of endogenous protoporphyrin in small cells [29], which is not supported by a model of oxygen diffusion [18].

Comparison of results reported for identical experimental models (e.g. isolated rat liver mitochondria or HUVEC; Table 1A, B) suggests that discrepancies of p_{50} are primarily related to methodological issues. The scatter of reported p_{50} values increased dramatically since 2003 (Fig. 4). Consideration of fundamental instrumental and experimental criteria helps to discriminate between physiological variability and experimental bias (Fig. 3). In several cases, separation of facts and artefacts on oxygen kinetics is impossible without extending the studies in question by methodological tests, particularly variation of mitochondrial or cell density (Fig. 2; [12, 13]).

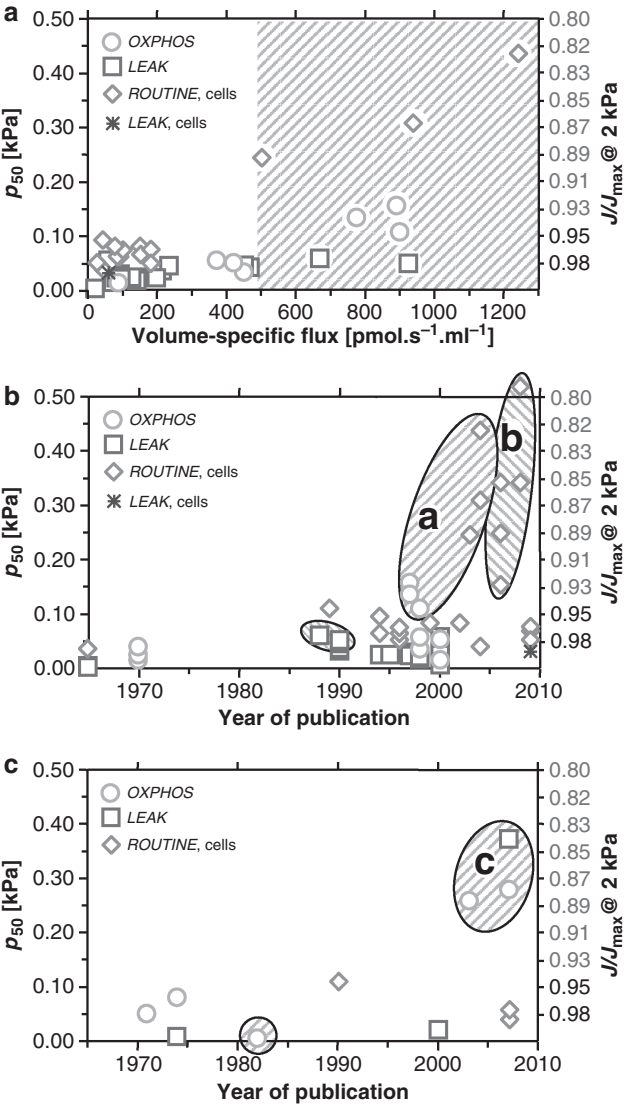

Fig. 4 p_{50} for respiration of isolated, coupled mitochondria and intact small cells. **a**: p_{50} measured in closed, well stirred respirometry chambers with aerobic-anoxic transitions as a function of volume-specific oxygen flux. The critical range >500 pmol·s^{-1}·ml^{-1} is hatched. **b**: Closed systems; hatched areas (**a**) high volume-specific flux, correspondingly fast aerobic-anoxic transitions and insufficient time resolution (Fig. 3c), and (**b**) EPR oxymetry without stirring. **c**: Open systems; hatched areas (**c**) indicate results obtained with an identical GAP instrument including a gas phase. Experimental details and references in Table 1

4.2 Methodological Limitations of Closed Systems

The basis of oxygen kinetic measurements in closed respirometry systems [30] is the measurement of oxygen flux in aerobic-anoxic transitions (Fig. 1). To compensate for low instrumental resolution, high mitochondrial concentrations (>0.2 mg mitochondrial protein/ml) have been used to achieve accurate measurement of oxygen flux. Under these conditions, rapid aerobic-anoxic transitions present a potential problem as pointed out by Britton Chance more than 40 years ago: "It is probable that the enzyme concentrations were so high under our experimental conditions that the enzyme passed too rapidly through the first order region for an accurate measurement of the K_m value" [10]. Direct experimental evidence for the magnitude of such inaccuracies was provided by using a large range of mitochondrial densities for measurement of oxygen kinetics [13]. Volume-specific oxygen flux is shown as a function of oxygen pressure at increasing protein concentrations of isolated rat heart mitochondria (Fig. 3). The p_{50} is 0.035 kPa in the active *OXPHOS* state, as measured at protein concentrations ranging from 0.02 to 0.12 mg/ml (Fig. 3a,b). At higher mitochondrial concentrations, volume-specific fluxes >500 $\text{pmol}\cdot\text{s}^{-1}\cdot\text{ml}^{-1}$ result in artificially high p_{50} values (Fig. 3c).

Correction of the oxygen signal for the exponential time constant of the POS [3] is important but insufficient at high flux when the aerobic-anoxic transition time is too short (Fig. 4a). At densities of 0.2–0.5 mg/ml (25°C) of rat liver and heart mitochondria in the passive *LEAK* state, volume-specific fluxes are in the range of 50–100 $\text{pmol}\cdot\text{s}^{-1}\cdot\text{ml}^{-1}$, which are optimum for oxygen kinetics and result in a reproducible p_{50} of 0.02 kPa [3, 27, 31, 32] (Table 1A). In contrast, even high-resolution respirometry cannot resolve short transition times <30–40 s from 10 μM to zero oxygen at high volume-specific flux >500 $\text{pmol}\cdot\text{s}^{-1}\cdot\text{ml}^{-1}$ in closed chambers, which explains the erroneously high p_{50} of 0.15 kPa for rat liver and heart mitochondria [32] respiring in the active *OXPHOS* state (Table 1B; Fig. 4a).

Varying human umbilical vein endothelial cell (HUVEC) density in a three-fold range from $0.6\cdot10^6$ to $2.0\cdot10^6$ cells/ml, maximum oxygen flow and p_{50} of *ROUTINE* respiration vary by a factor of 1.4, from 35 to 49 $\text{pmol}\cdot\text{s}^{-1}\cdot10^{-6}$ and from 0.052 to 0.075 kPa, respectively, in endothelial growth medium without inhibitor [12]. In contrast, a 6-fold higher p_{50} of 0.44 kPa was reported for HUVEC in the presence of L-NMMA (NOS inhibitor) with $31\cdot10^6$ cells/ml and corresponding high volume-specific flux [33]. Instruments with high O_2 back-diffusion [33, 34] are particularly sensitive to artefacts of rapid aerobic-anoxic transitions (Fig. 4a).

In electron paramagnetic resonance (EPR) oxymetry, small numbers of cells can be studied in micro chambers of 50 μl volume [35]. Without sufficient stirring, oxygen gradients develop in diffusion zones around cells [35], comparable to the diffusion zone towards the POS membrane [36]. Although diffusion conditions across unstirred POS are simpler to model in comparison to

suspended cells, corrections are inherently inaccurate and the only satisfactory solution for measurement of dissolved oxygen is obtained by vigorous stirring, as in HRR. Taking oxygen diffusion in unstirred EPR oxymetry into consideration reduces the estimate of p_{50} for respiration of endothelial cells two-fold [35], but the corrected p_{50} values remain highly sensitive to cell density ($2 \cdot 10^6$–$5 \cdot 10^6$ cells/ml; Table 1B). The minimum oxygen pressure, $p^{\#}$, at which cessation of respiration in EPR oxymetry indicates equilibrium to be established within mitochondria, is at 0.05 kPa [35] (in the range of p_{50} from HRR), whereas the thermodynamic equilibrium p_{O_2} is 0.0003 kPa for coupled mitochondrial oxygen reduction [3]. Perhaps oxygen diffusion through the tube sealing clay contributes to the high $p^{\#}$ in capillaries used for EPR oxymetry. The sensitivity (>2-fold) of $p^{\#}$ on diffusion corrections indicates that it is not a thermodynamic equilibrium property, since diffusion gradients are dissipated in the approach to equilibrium. Further uncertainties may result from high noise of flux and lack of temperature control in EPR oxymetry. The diffusion model applied for correction in EPR oxymetry assumes that the diffusion zone increases as a steady function of time [35], whereas experimental validation – using the POS as a test system – suggests that a steady-state is reached after a short period of a few minutes. Wall effects are not considered, nor potential effects of cell aggregation in the confinement of a 50 µl capillary [35]. Taken together, these difficulties may explain the high apparent p_{50} derived from EPR oxymetry (Fig. 4b).

4.3 Variation of p_{50} in Open Systems

Using a steady-state approach with oxygen transfer from the gas to aqueous phase (GAP), Sugano et al. [21] report a p_{50} of 0.08 kPa in active pigeon heart mitochondria at a protein concentration of 0.2 mg/ml (Table 1A). At 10 mg/ml, however, Cole et al. [37] obtained a p_{50} of 0.005 kPa in active rat skeletal muscle mitochondria. Using the identical instrumental GAP respirometry system, a p_{50} of 0.37 kPa was reported for rat liver mitochondria in the passive *LEAK* state [38], 75 times higher than in ADP-stimulated rat skeletal muscle mitochondria [37] (Fig. 4c). In contrast to the well established direct proportionality between p_{50} and turnover of cytochrome *c* oxidase [10–13, 22, 26, 28], the p_{50} obtained by GAP respirometry was paradoxically higher in the quiescent *LEAK* state compared to the active *OXPHOS* state [38]. GAP respirometry, therefore, yields inconsistent results on mitochondrial oxygen kinetics (Fig. 4c). Under conditions of very high flux [37], oxygen gradients between the gas and aqueous phases and towards the oxygen sensor at the bottom of the chamber may explain differences between the mitochondrial response to oxygen pressure in the heterogeneous system and the much lower p_{50} reported by the POS in GAP respirometry. This does not explain, however, why the reported p_{50} increases as the volume specific flux declines in this GAP respirometric system (Table 1B).

In addition, previous claims that the p_{50} may be lower in closed than open systems [39] are rejected with reference to the literature summarized over the past 40 years in general and to discrepancies of GAP respirometry in particular (Fig. 4, Table 1).

4.4 Variation of p_{50} In Vivo

Living cells provide an in vivo model that can be studied *in vitro*, both in closed measuring systems or open systems at steady state. The p_{50} of mitochondrial respiration in vivo varies as a function of metabolic state (turnover of cytochrome *c* oxidase), as observed in living cells (Fig. 2). The ^{1}H nuclear magnetic resonance signal of deoxymyoglobin provides an elegant means of monitoring intracellular oxygen saturation in vivo, reducing Δp_{50} (Eq. 2) to the effects of intracellular oxygen gradients. Using this approach in perfused rat heart [40], maximally active human skeletal muscle [41] and mouse skeletal muscle at rest or stimulated by uncoupling [42], p_{50} values of mitochondrial respiration range from 0.07 to 0.2 kPa (Table 1C), whereas the p_{50} in resting rat cardiomyocytes is 0.015 based on intracellular p_{O_2} derived from spectrophotometric myoglobin saturation measurements [43]. The dependence of cellular or tissue respiration on average myoglobin saturation does not accurately reflect the p_{50} of mitochondrial respiration. Direct comparison would require modelling of the distribution of mitochondria [44] over the range of local oxygen pressures as determined by intracellular oxygen gradients [4], and particularly evaluation of anoxic core regions [5] and their effect on the overall response of tissue or cell respiration under these heterogeneous oxygen conditions. A mitochondrial p_{50} of 0.067 has been derived from a model of brain oxygen supply [45].

5 Conclusions

The p_{50} of mitochondrial respiration in the range of 0.02–0.05 kPa (0.15–0.4 mmHg) indicates close matching of the affinity of cytochrome *c* oxidase to the demands imposed on enzyme function in the low-oxygen environment within cells. 86% myoglobin saturation (2 kPa O_2) in normoxic resting mouse skeletal muscle [42] supports full (99%) respiratory capacity of mitochondria in the *LEAK* state (Table 1A). At maximum aerobic exercise in human muscle, however, myoglobin saturation is 50% ($p_{O_2} = 0.3$–0.4 kPa) [41, 46], which implies an oxygen limitation to 0.9 of maximum mitochondrial capacity, assuming homogenous oxygen distribution. Short-term performance at the extreme of maximum aerobic muscle power induces physiological, intracellular hypoxia at environmental normoxia, if we consider oxygen limitation by $>5\%$ as a criterion of defining bioenergetic hypoxia.

In contrast, with a p_{50} as high as 0.4 kPa (3 mmHg; Table 1B), mitochondrial activity would be limited to 0.44 of respiratory capacity at 50% myoglobin saturation. Even at an intracellular oxygen pressure of 4–5 kPa in liver [47], respiration rate would reach only 0.9 of capacity. Such high p_{50} values of mitochondrial respiration are experimental artefacts resulting from high volume-specific flux in closed chambers (Fig. 4a) and of diffusion limitation in unstirred systems (Fig. 4b). Internally inconsistent results on p_{50} from open GAP respirometry indicate a methodological problem which remains unresolved (Fig. 4c). Several recent studies on the inhibition of cytochrome *c* oxidase by NO report erroneously high p_{50} in the absence of inhibitor [33, 34, 39]. A critical evaluation is required whether or not these methodological deficiencies extend into the higher oxygen range where NO inhibits cytochrome *c* oxidase, a compensatory shift may occur of cytochrome redox states [33, 48] and mitochondrial ROS production may be affected.

At half-maximum aerobic power, myoglobin saturation in skeletal muscle is increased to 70% ($p_{O_2} = 0.9$ kPa [46]), corresponding to oxygen limitation of 5% with a p_{50} of 0.05 kPa. An intracellular p_{O_2} of 1–2 kPa at modest routine activity, therefore, is the normoxic mitochondrial microenvironment in skeletal muscle, and the high affinity of mitochondrial respiration for oxygen prevents significant oxygen limitation under these conditions. On the other hand, a p_{50} of 0.02–0.05 kPa is not excessively low and thus provides the potential for mitochondria to function as a bioenergetic oxygen sensor and playing a role in oxygen signalling and adaptation to hypoxia [49, 50].

Acknowledgments We thank Prof. Dr. Jakob Troppmair for providing the 32D and 32D-vRAF cell lines.

References

1. Weibel ER, Taylor CR, Hoppeler H (1991) The concept of symmorphosis: a testable hypothesis of structure-function relationship. Proc Natl Acad Sci USA 88:10357–10361.
2. Gnaiger E, Lassnig B, Kuznetsov AV et al. (1998) Mitochondrial oxygen affinity, respiratory flux control and excess capacity of cytochrome *c* oxidase. J Exp Biol 201:1129–1139.
3. Gnaiger E, Steinlechner-Maran R, Méndez G et al. (1995) Control of mitochondrial and cellular respiration by oxygen. J Bioenerg Biomembr 27:583–596.
4. Takahashi E, Endoh H, Doi K (2000) Visualization of myoglobin-facilitated mitochondrial O_2 delivery in a single isolated cardiomyocyte. Biophys J 78:3252–3259.
5. Takahashi E (2008) Anoxic cell core can promote necrotic cell death in cardiomyocytes at physiological extracellular PO_2. Am J Physiol Heart Circ Physiol 294:H2507–H2515.
6. Gnaiger E (2003) Oxygen conformance of cellular respiration. A perspective of mitochondrial physiology. Adv Exp Med Biol 543:39–55.
7. Chance B, Williams GR (1955) Respiratory enzymes in oxidative phosphorylation. III. The steady state. J Biol Chem 217:409–427.
8. Puchowicz MA, Varnes ME, Cohen BH et al. (2004) Oxidative phosphorylation analysis: assessing the integrated functional activity of human skeletal muscle mitochondria-case studies. Mitochondrion 4:377–385.

9. Gnaiger E, ed (2007) Mitochondrial pathways and respiratory control. OROBOROS MiPNet Publications, Innsbruck.
10. Chance B (1965) Reaction of oxygen with the respiratory chain in cells and tissues. J Gen Physiol 49:163–195.
11. Gnaiger E (2001) Bioenergetics at low oxygen: dependence of respiration and phosphorylation on oxygen and adenosine diphosphate supply. Respir Physiol 128:277–297.
12. Steinlechner-Maran R, Eberl T, Kunc M et al. (1996) Oxygen dependence of respiration in coupled and uncoupled endothelial cells. Am J Physiol 271:C2053–C2061.
13. Gnaiger E, Lassnig B, Kuznetsov AV, Margreiter R (1998) Mitochondrial respiration in the low oxygen environment of the cell. Effect of ADP on oxygen kinetics. Biochim Biophys Acta 1365:249–254.
14. Hütter E, Renner K, Pfister G, Stöckl P et al. (2004) Senescence-associated changes in respiration and oxidative phosphorylation in primary human fibroblasts. Biochem J 380:919–928.
15. Gnaiger E (2008) Polarographic oxygen sensors, the oxygraph, and high-resolution respirometry to assess mitochondrial function. In: Dykens JA, Will Y (ed) Mitochondrial dysfunction in drug-induced toxicity. Wiley, New York.
16. Renner K, Amberger A, Konwalinka G et al. (2003) Changes of mitochondrial respiration, mitochondrial content and cell size after induction of apoptosis in leukemia cells. Biochim Biophys Acta 1642:115–123.
17. Schindler FJ (1967) Determination of oxygen affinity. Methods Enzymol 10:629–634.
18. Rumsey WL, Schlosser C, Nuutinen EM et al. (1990) Cellular energetics and the oxygen dependence of respiration in cardiac myocytes isolated from adult rat. J Biol Chem 265:15392–15402.
19. Cornish-Bowden A (1995) Fundamentals of enzyme kinetics. Portland Press, London.
20. Troppmair J, Rapp UR (2003) Raf and the road to cell survival: a tale of bad spells, ring bearers and detours. Biochem Pharmacol 66:1341–1345.
21. Sugano T, Oshino N, Chance B (1974) Mitochondrial functions under hypoxic conditions. The steady states of cytochrome *c* reduction and of energy metabolism. Biochim Biophys Acta 347:340–358.
22. Verkhovsky MI, Morgan JE, Puustinen A, Wikström M (1996) Kinetic trapping of oxygen in cell respiration. Nature 380:268–270.
23. Riistama S, Puustinen A, García-Horsman A et al. (1996) Channelling of dioxygen into the respiratory enzyme. Biochim Biophys Acta 1275:1–4.
24. Hütter E, Renner K, Jansen-Dürr P, Gnaiger E (2002) Biphasic oxygen kinetics of cellular respiration and linear oxygen dependence of antimycin A inhibited oxygen consumption. Mol Biol Rep 29:83–87.
25. Pecina P, Gnaiger E, Zeman J et al. (2004) Decreased affinity for oxygen of cytochrome-*c* oxidase in Leigh syndrome caused by SURF1 mutations. Am J Physiol Cell Physiol 287:C1384–C1388.
26. Laisk A, Oja V, Eichelmann H (2007) Kinetics of leaf oxygen uptake represent in planta activities of respiratory electron transport and terminal oxidases. Physiol Plant 131:1–9.
27. Gnaiger E, Mendez G, Hand SC (2000) High phosphorylation efficiency and depression of uncoupled respiration in mitochondria under hypoxia. Proc Natl Acad Sci USA 97:11080–11085.
28. St-Pierre J, Tattersall GJ, Boutilier RG (2000) Metabolic depression and enhanced O_2 affinity of mitochondria in hypoxic hypometabolism. Am J Physiol Regul Integr Comp Physiol 279:R1205–R1214.
29. Mik EG, Stap J, Sinaasappel M et al. (2006) Mitochondrial PO_2 measured by delayed fluorescence of endogenous protoporphyrin IX. Nature Methods 3:939–945.
30. Longmuir IS (1957) Respiration rate of rat-liver cells at low oxygen concentrations. Biochem J 65:378–382.

31. Mendez G, Gnaiger E (1994) How does oxygen pressure control oxygen flux in isolated mitochondria? A methodological approach by high-resolution respirometry and digital data analysis. In Gnaiger E, Gellerich FN, Wyss M (ed) What is controlling life? Modern Trends BioThermoKinetics, Innsbruck University Press, Innsbruck.
32. Costa LE, Mendez G, Boveris A (1997) Oxygen dependence of mitochondrial function measured by high-resolution respirometry in long-term hypoxic rats. Am J Physiol 273:C852–C858.
33. Palacios-Callender M, Quintero M, Hollis VS et al. (2004) Endogenous NO regulates superoxide production at low oxygen concentrations by modifying the redox state of cytochrome *c* oxidase. Proc Natl Acad Sci USA 101:7630–7635.
34. Hollis VS, Palacios-Callender M, Springett RJ et al. (2003) Monitoring cytochrome redox changes in the mitochondria of intact cells using multi-wavelength visible light spectroscopy. Biochim Biophys Acta 1607:191–202.
35. Presley T, Kuppusamy P, Zweier JL, Ilangovan G (2006) Electron paramagnetic resonance oximetry as a quantitative method to measure cellular respiration: a consideration of oxygen diffusion interference. Biophys J 91:4623–4631.
36. Gnaiger E, Forstner H (1983) Polarographic Oxygen Sensors. Aquatic and Physiological Applications. Springer, Berlin.
37. Cole RC, Sukanek PC, Wittenberg JB, Wittenberg BA (1982) Mitochondrial function in the presence of myoglobin. J Appl Physiol 53:1116–1124.
38. Hoffman DL, Salter JD, Brookes PS (2007) Response of mitochondrial reactive oxygen species generation to steady-state oxygen tension: implications for hypoxic cell signaling. Am J Physiol Heart Circ Physiol 292:H101–H108.
39. Brookes PS, Kraus DW, Shiva S et al. (2003) Control of mitochondrial respiration by $NO^{\bullet}$, effects of low oxygen and respiratory state. J Biol Chem 278:31603–31609.
40. Kreutzer U, Jue T (1995) Critical intracellular O_2 in myocardium as determined by 1H nuclear magnetic resonance signal of myoglobin. Am J Physiol 268:H1675–H1681.
41. Richardson RS, Leigh JS, Wagner PD, Noyszewski EA (1999) Cellular PO_2 as a determinant of maximal mitochondrial O_2 consumption in trained human skeletal muscle. J Appl Physiol 87:325–331.
42. Marcinek DJ, Ciesielski WA, Conley KE, Schenkman KA (2003) Oxygen regulation and limitation to cellular respiration in mouse skeletal muscle in vivo. Am J Physiol Heart Circ Physiol 285:H1900–H1908.
43. Wittenberg BA, Wittenberg JB (1985) Oxygen pressure gradients in isolated cardiac myocytes. J Biol Chem 260:6548–6554.
44. Benard G, Rossignol R (2008) Ultrastructure of the mitochondrion and its bearing on function and bioenergetics. Antiox Redox Signaling 10:1313–1342.
45. Gjedde A, Johannsen P, Cold GE, Ostergaard L (2005) Cerebral metabolic response to low blood flow: possible role of cytochrome oxidase inhibition. J Cereb Blood Flow Metab 25:1183–1196.
46. Molé PA, Chung Y, Tran TK et al. (1999) Myoglobin desaturation with exercise intensity in human gastrocnemius muscle. Am J Physiol 277:R173–R180.
47. Mik EG, Johannes T, Zuurbier CJ et al. (2008) In vivo mitochondrial oxygen tension measured by a delayed fluorescence lifetime technique. Biophys J 95:3977–3990.
48. Arthur PG, Ngo C-T, Moretta P, Guppy M (1999) Lack of oxygen sensing by mitochondria in platelets. Eur J Biochem 266:215–219.
49. Kwast KE, Burke PV, Staahl BT, Poyton RO (1999) Oxygen sensing in yeast: evidence for the involvement of the respiratory chain in regulating the transcription of a subset of hypoxic genes. Proc Natl Acad Sci USA 96:5446–5451.
50. Fukuda R, Zhang H, Kim J-W et al. (2007) HIF-1 regulates cytochrome oxidase subunits to optimize efficiency of respiration in hypoxic cells. Cell 129:111–122.
51. Barzu O, Satre M (1970) Determination of oxygen affinity of respiratory systems using oxyhemoglobin as oxygen donor. Anal Biochem 36:428–433.

52. Degn H, Wohlrab H (1971) Measurement of steady-state values of respiration rate and oxidation levels of respiratory pigments at low oxygen tensions. A new technique. Biochim Biophys Acta 245:347–355.
53. Robiolio M, Rumsey WL, Wilson DF (1989) Oxygen diffusion and mitochondrial respiration in neuroblastoma cells. Am J Physiol 256:C1207–C1213.
54. Steinlechner R, Eberl T, Margreiter R, Gnaiger E (1994) Oxygen dependence of cellular respiration in endothelial cells: a sensitive toxicological test. In Gnaiger E, Gellerich FN, Wyss M (ed) What is controlling life? 50 years after Erwin Schrödinger's What is Life? Innsbruck University Press, Innsbruck.
55. Mertens S, Noll T, Spahr R et al. (1990) Energetic response of coronary endothelial cells to hypoxia. Am J Physiol 258:H689–H694.
56. Wilson DF, Rumsey WL, Green TJ, Vanderkooi J (1988) The oxygen dependence of mitochondrial oxidative phosphorylation measured by a new optical method for measuring oxygen concentration. J Biol Chem 263:2712–2718.
57. Jones CI, Han Z, Presley T et al. (2008) Endothelial cell respiration is affected by the oxygen tension during shear exposure: role of mitochondrial peroxynitrite. Am J Physiol Cell Physiol 295:C180–C191.

http://www.springer.com/978-1-4419-1239-8

Oxygen Transport to Tissue XXXI
(Eds.)E. Takahashi; D.F. Bruley
2010, XXXVIII, 516 p. 179 illus., 15 in color., Hardcover
ISBN: 978-1-4419-1239-8